Efficiency of Polyoxometalates-Based Mesoporous Hybrids as Covalently Anchored Catalysts

Faiza Bentaleb; Ourania Makrygenni; Dalil Brouri; Cristina Coelho Diogo, Ahmad Mehdi, Anna Proust; Franck Launay; Richard Villanneau

Supplementary Informations

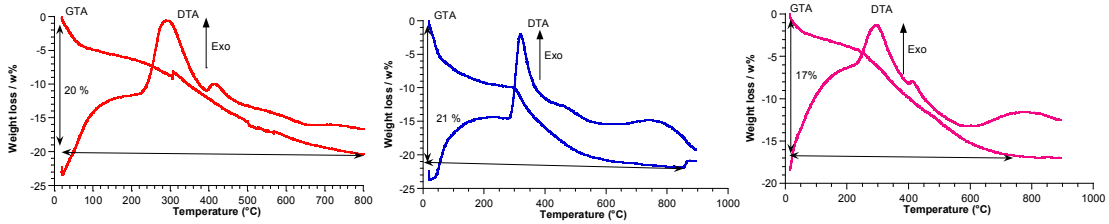

Fig. S1 Thermogravimetric analysis (TGA), weight loss (wt%) and DTA curve of SBA-NH_2 (red), SBA-COOH (blue) and MCF-NH_2 (pink).

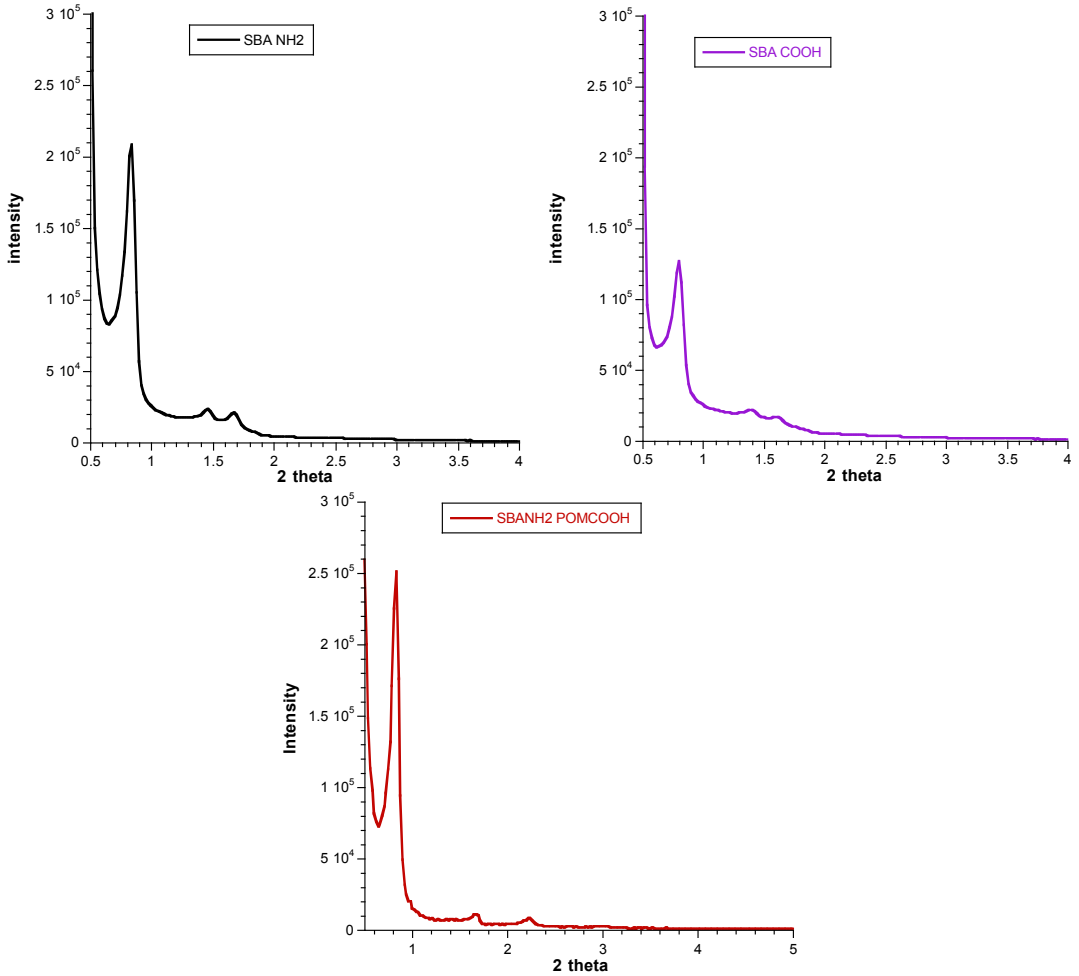

Fig. S2: Powder X-ray diffraction patterns of SBA-NH_2 (black), SBA-CO_2H (purple) and POM-CO_2H@SBA-NH_2 (red).

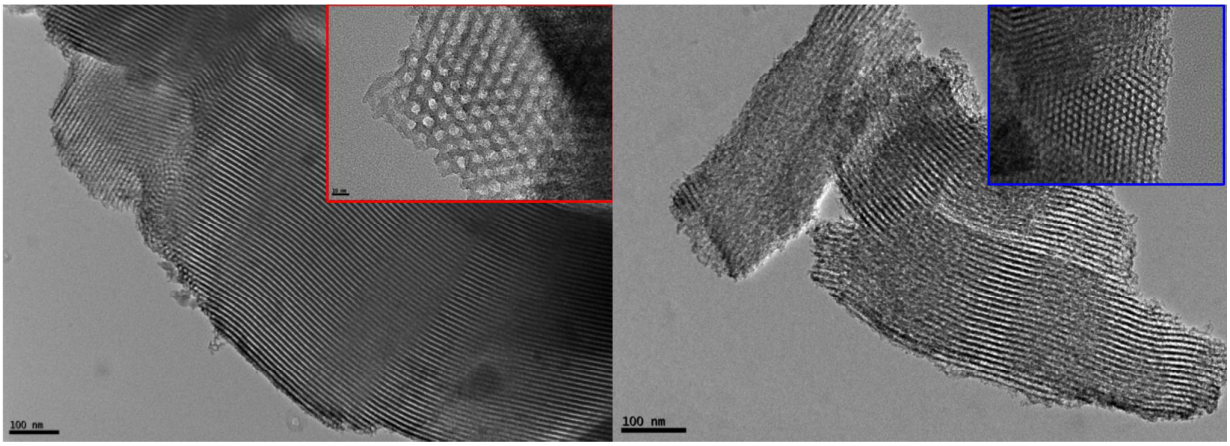

Fig. S3: TEM micrographs of SBA-NH_2 (left) and SBA-COOH materials (right).

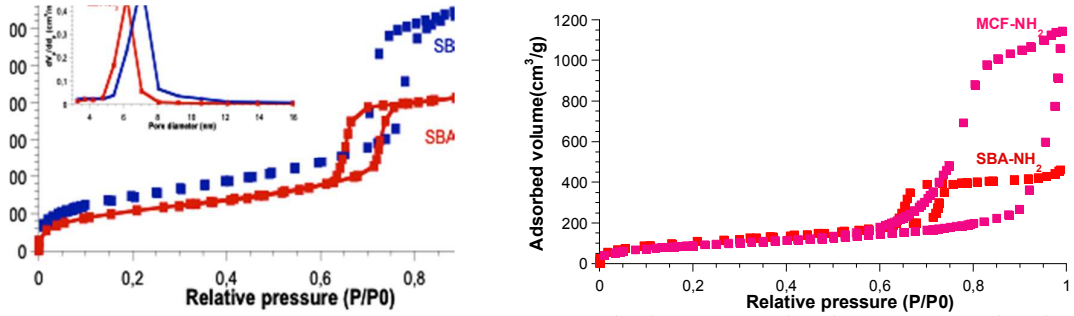

Fig. S4: Nitrogen adsorption/desorption isotherms of SBA-NH_2 (red), SBA-CO_2H (blue) and MCF-NH_2 (pink). BJH pore-size distributions for SBA-NH_2 and SBA-CO_2H were calculated from the desorption branch.

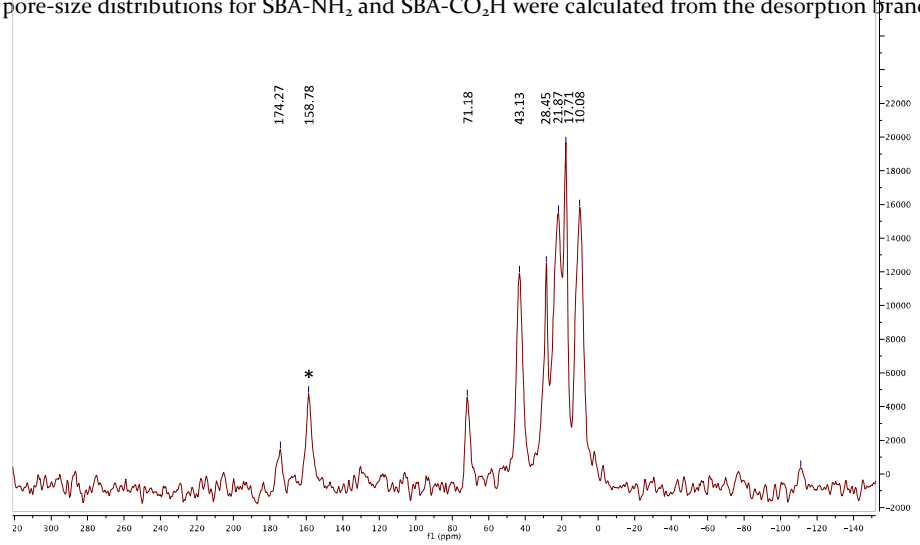

Fig. S5: ^{13}C CP-MAS NMR spectrum of POM-CO_2H@MCF-NH_2. The peak at 174.27 ppm corresponds to C atoms of the carbonyle functions of the amide groups formed after coupling reactions. The peak with an asterisk (*) corresponds to isobutylchloroformiate that has not been correctly removed in the present sample.

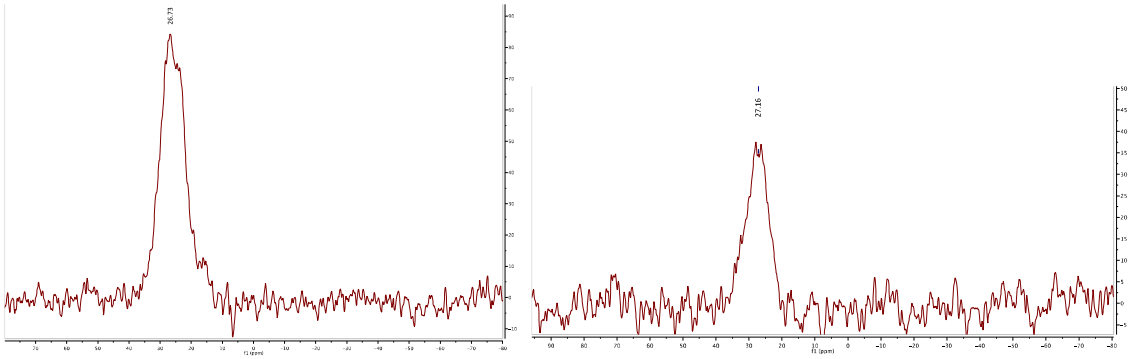

Fig. S6: ^{31}P CP-MAS NMR spectra of POM-CO_2H@SBA-NH_2 (left) and POM-CO_2H@MCF-NH_2 (right). In both materials, we observed one large signal centred at 26.73 and 27.16 ppm, respectively, corresponding to the {R<u>P</u>=O} functions of the grafted organophosphonyle derivative of POM (POM-CO_2H), in accordance with the work previously described.

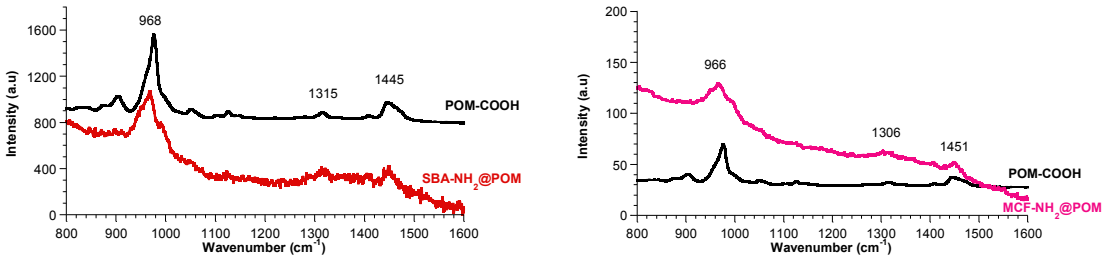

Fig. S7: Raman spectra of POM-CO_2H@SBA-NH_2 (red) and POM-CO_2H@MCF-NH_2 (pink) compared to that of TBA_3NaH(**1**) (black)

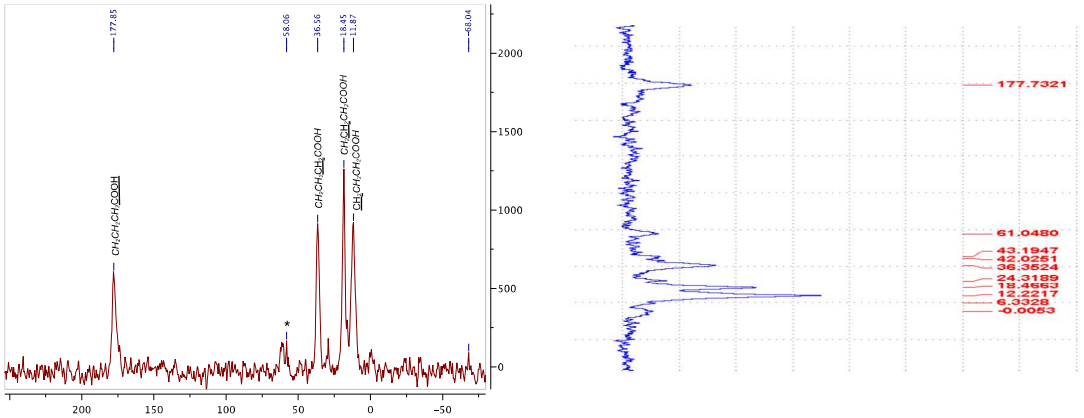

Fig. S8: ^{13}C CP-MAS NMR spectrum of SBA-COOH and of POM-NH_2 @SBA-CO_2H.

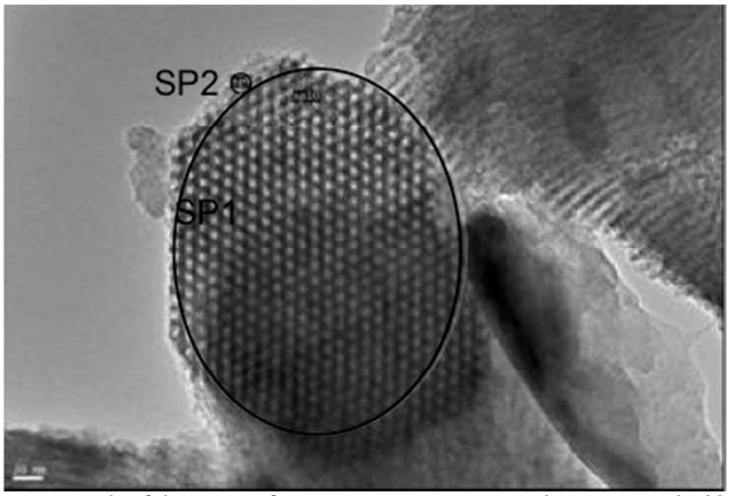

	SP1 (%)	SP2 (%)
W	4.7	7.8
Si	29.7	26.8
W/Si	0.16	0.29

Fig. S9: Details of the zones of a POM-CO_2H@SBA-NH_2 silica grain studied by XEDS and table indicating the W/Si contents in the whole grain (SP1) and inside a channel (SP2) after deconvolution of the XEDS spectrum.

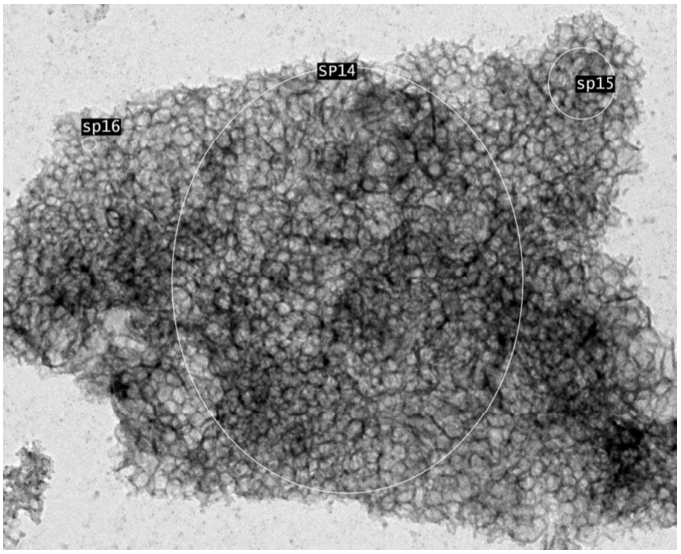

	SP14 (%)	SP15 (%)	SP16 (%)
W	3.7	3.2	8.4
Si	23.2	23.8	27.6
W/Si	0.16	0.13	0.30

Fig. S10: Details of the zones of a POM-CO_2H@MCF-NH_2 silica grain studied by XEDS and table indicating the W/Si contents in the whole grain (SP14), part of the grain (SP15) and inside a cell (SP16) after deconvolution of the XEDS spectrum.

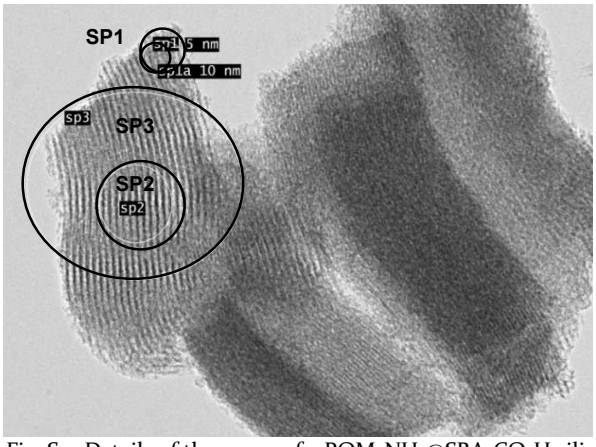

	SP1 (%)	SP1a (%)	SP2 (%)	SP3 (%)
W	2.1	1.5	1.3	1.1
Si	43.5	44.7	41.8	38.6
W/Si	0.048	0.033	0.031	0.028

Fig. S11: Details of the zones of a POM-NH_2@SBA-CO_2H silica grain studied by XEDS and table indicating the W/Si contents in the whole grain (SP3), part of the grain (SP2 and SP1a) and inside a channel (SP1) after deconvolution of the XEDS spectrum.